

Fortnightly modulation of San Andreas tremor and low-frequency earthquakes

Nicholas J. van der Elst^{a,1}, Andrew A. Delorey^b, David R. Shelly^c, and Paul A. Johnson^b

^aEarthquake Science Center, US Geological Survey, Pasadena, CA 91106; ^bGeophysics Group, Los Alamos National Laboratory, Los Alamos, NM 87545; and ^cVolcano Science Center, US Geological Survey, Menlo Park, CA 94025

Edited by Thorne Lay, University of California, Santa Cruz, CA, and approved June 10, 2016 (received for review December 9, 2015)

Earth tides modulate tremor and low-frequency earthquakes (LFEs) on faults in the vicinity of the brittle–ductile (seismic–aseismic) transition. The response to the tidal stress carries otherwise inaccessible information about fault strength and rheology. Here, we analyze the LFE response to the fortnightly tide, which modulates the amplitude of the daily tidal stress over a 14-d cycle. LFE rate is highest during the waxing fortnightly tide, with LFEs most strongly promoted when the daily stress exceeds the previous peak stress by the widest margin. This pattern implies a threshold failure process, with slip initiated when stress exceeds the local fault strength. Variations in sensitivity to the fortnightly modulation may reflect the degree of stress concentration on LFE-producing brittle asperities embedded within an otherwise aseismic fault.

faults | low-frequency earthquakes | tidal triggering | fortnightly tides

Solid Earth tides trigger both earthquakes and tectonic tremor. Tidal triggering of earthquakes is found only for select environments, including shallow thrust faults (1, 2) and midoceanic ridges and transforms (3–5). Tidal triggering of tremor, on the other hand, has been found almost everywhere that tectonic tremor is observed (6–10). Tidal triggering acts as a probe of the properties of faults at depth, generating insights into the mechanics of the brittle–ductile transition (11–16).

Tectonic tremor is believed to result from the superposition of many low-frequency earthquakes (LFEs) occurring on seismic asperities imbedded in an aseismic or creeping medium (17–19). Individual LFE families (spatially localized patches of repeating LFEs) show varying sensitivity to tidal stresses, reflecting heterogeneities in the local stress state, pore pressure, frictional rheology, or other properties (12, 13).

Previous studies have analyzed the amplitude and phase of the semidiurnal tidal modulation of tremor on the San Andreas fault near Parkfield, CA (12, 13) (Fig. 1). Peak LFE rate coincides with the peak semidiurnal shear stress (12). The semidiurnal shear stress is only a few hundred Pascals—six orders of magnitude smaller than the lithostatic stress at the tremor depth of 16–30 km. These observations suggest a very weak fault with high pore pressure and poorly drained hydrologic conditions (12, 13).

The short-period nature of the semidiurnal tides complicates the physical interpretation of triggered LFEs, because the short-term response may be influenced by the time-dependent process of LFE nucleation (13, 20, 21) or by fault weakening as the tremor episode accelerates (16). To shed additional light on the mechanics of triggering for LFEs and creep episodes, we here analyze the effect of the fortnightly tides, which modulate the semidiurnal tidal amplitude on a 14-d cycle and are relatively far removed from the timescale of LFE nucleation.

Fortnightly modulation has been anticipated, but only recently found, for tectonic earthquakes (22, 23), and it has not yet been investigated for LFEs. The fortnightly tidal cycle can be thought of as the beat frequency arising from the interference between solar and lunar tides. The strongest (spring) tides occur when the moon and sun are aligned, and the weakest (neap) tides occur when the sun and moon are separated by 90°. This pattern results in a ~14-d modulation of the semidiurnal tidal amplitude (Fig. 24).

There are two fundamental ways by which the fortnightly cycle may affect LFE rate, both of which we document in the LFE catalog. The first effect is through the modulation of the amplitude of the peaks and troughs of the semidiurnal tides. Because LFEs correlate more strongly with larger-amplitude shear stress, both the minimum and maximum LFE rates should coincide with the fortnightly peak amplitudes (with ~0° phase lag). We refer to this as the amplitude effect. Unless the LFE response to positive and negative tides is asymmetrical [which it may be (13, 16)], the 0° fortnightly amplitude effect should average out to be essentially nil on timescales longer than a day.

The second way the fortnightly cycle may modulate LFE occurrence is by modulating the envelope of peak stress (Fig. 24). When combined with the secular tectonic loading rate, the fortnightly tide controls the amount by which the peak stress in each semidiurnal cycle exceeds the peak stress in all previous cycles. This “threshold” effect will show up as enhanced LFE activity during the waxing phase of the fortnightly tide (–90° phase), when the peak stress is most substantially exceeded in each cycle, followed by diminished activity during the waning phase.

Results and Discussion

Amplitude and Phase of the Tidal Modulation. We compute the tidal phase ϕ at the time of occurrence of each LFE. The phase is defined to be 0° at the peak tidal amplitude for both semidiurnal and fortnightly tides, ranging from –180° at the preceding minimum to 180° at the next (1) (Fig. 24).

Examining all LFE families together, we confirm a 23% semidiurnal modulation of LFE rate (12) with P value $\ll 0.01$ by Schuster’s test (24). The peak LFE rate has a phase lag of $19^\circ \pm 5^\circ$

Significance

The sun and moon exert a gravitational tug on Earth that stretches and compresses crustal rocks. This cyclic stressing can promote or inhibit fault slip, particularly at the deep roots of faults. The amplitude of the solid Earth tide varies over a fortnightly (2-wk) cycle, as the sun and moon change their relative positions in the sky. In this study, we show that deep, small earthquakes on the San Andreas Fault are most likely to occur during the waxing fortnightly tide—not when the tidal amplitude is highest, as might be expected, but when the tidal amplitude most exceeds its previous value. The response of faults to the tidal cycle opens a window into the workings of plate tectonics.

Author contributions: N.J.v.d.E., A.A.D., D.R.S., and P.A.J. designed research; N.J.v.d.E. performed research; D.R.S. collected and reduced the seismological data; N.J.v.d.E. performed the tidal analysis; N.J.v.d.E., A.A.D., D.R.S., and P.A.J. analyzed data; and N.J.v.d.E., A.A.D., D.R.S., and P.A.J. wrote the paper.

The authors declare no conflict of interest.

This article is a PNAS Direct Submission.

¹To whom correspondence should be addressed. Email: nvanderelst@usgs.gov.

This article contains supporting information online at www.pnas.org/lookup/suppl/doi:10.1073/pnas.1524316113/-DCSupplemental.

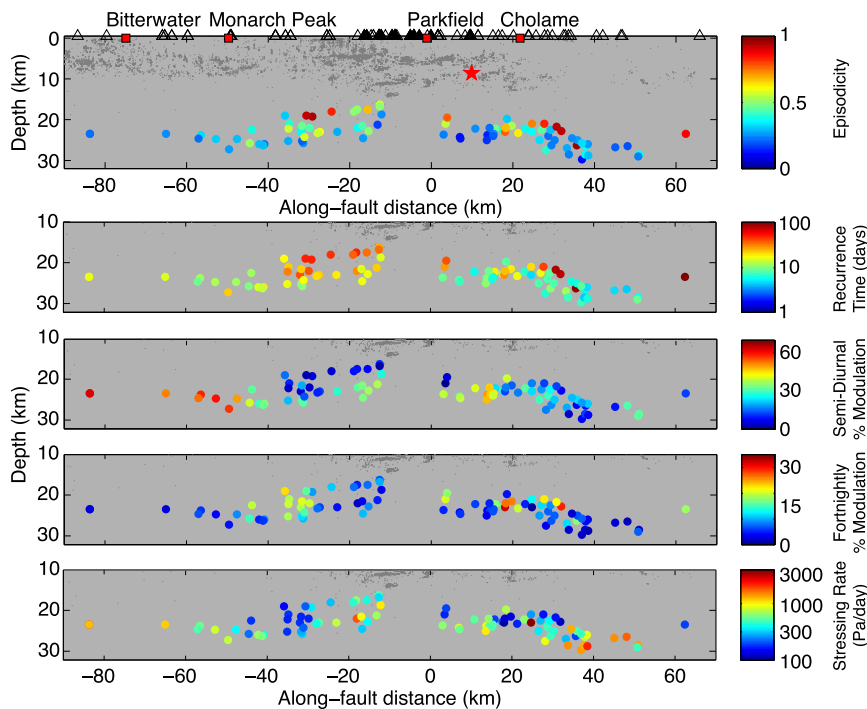


Fig. 4. Cross-sections of measured and estimated parameters for LFE families on the San Andreas Fault. Northwest is to the left. Colored dots are LFE families; small gray dots are upper crustal earthquakes. The red star is the 2004 Parkfield earthquake hypocenter. Seismic stations are marked by triangles.

threshold failure, but are driven indirectly by tidally modulated creep in the encompassing fault zone, which results in the overall rate being again in phase with the tidal stress (12, 13, 16). The latter model is consistent with the pulse-like quality of the LFE episodes, and with observations in other regions (e.g., Cascadia) that find a correspondence between tremor and geodetically observed slow slip (12, 13, 16).

Regardless of which semidiurnal triggering model is correct, the inverse relationship between the strength of the semidiurnal and fortnightly modulations provides a key insight into the mechanics of LFEs and the structure of the deep fault. Based on the phase of the two tidal correlations, we infer that the amplitude of the fortnightly modulation reflects variations in stress concentration on LFE asperities, and the amplitude of the semidiurnal modulation reflects variations in overall fault strength. The more continuous LFE families have high semidiurnal sensitivity and low fortnightly sensitivity, suggesting low overall fault strength and high apparent stressing rate (high stress concentration). These two observations are consistent with the more continuous LFEs being generated on isolated asperities within an otherwise aseismic, weak creeping fault zone. The more episodic families, on the other hand, have low semidiurnal sensitivity and high fortnightly sensitivity, suggesting higher overall fault strength and lower stress concentration. This pattern is consistent with larger, more contiguous LFE asperities.

Overall, the observations paint a picture consistent with the idea that the brittle–ductile transition is gradational and heterogeneous, with LFE-producing asperities becoming smaller and more isolated as the transition to aseismic deformation becomes more complete. The inverse relationship between the LFE responses observed at two different tidal timescales should serve as a powerful constraint on future models of the rheology and mechanics of the deep San Andreas.

Materials and Methods

Calculation of the Tidal Shear Stress. We use Duncan Agnew's tidal code package SPOTL (subroutine *ertid*) to calculate the solid Earth tides (28). This

subroutine computes tides for the second and third lunar harmonics and the second solar harmonic, which is adequate, given our focus on the average response at semidiurnal and fortnightly periods. The ocean loading component can be neglected for this section of the San Andreas (10). We assume that the coefficient of friction is near zero, based on previous estimates (10) of $\mu = 0.02$, and look only at the fault-parallel shear stress in the semidiurnal tidal analysis. The fortnightly tide modulates all components of the tidal stress, and is therefore not specific to any particular component.

In computing fault shear stress, we assume linear elasticity, plane strain, a Poisson's ratio of 0.25, and a shear modulus of 30 GPa. We resolve the tidal shear stress on a vertically dipping, right-lateral fault with azimuth 315° . Because the fortnightly cycle modulates all components of the tidal strain

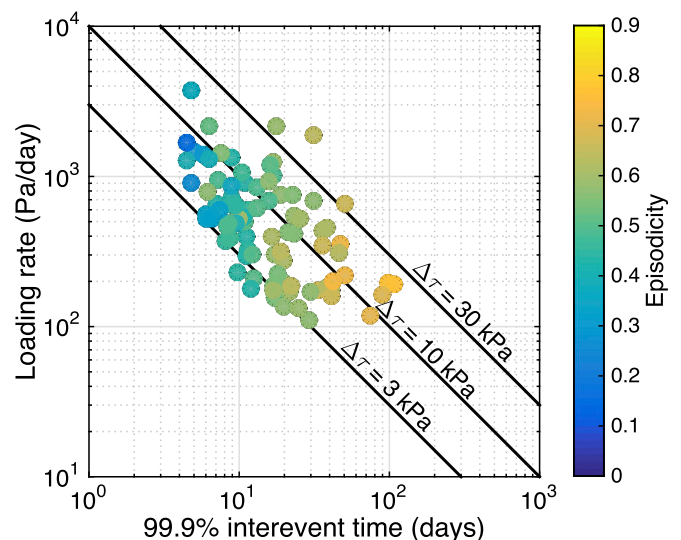


Fig. 5. Loading rate estimated from the amplitude of the fortnightly modulation, against maximum recurrence time for each LFE family. Black lines are contours of constant stress accumulation (stress drop) per episode.

tensor in the same way, there should be minimal sensitivity to small inaccuracies in the stress tensor (22). Unfortunately, this insensitivity also limits our ability to measure the relative contributions of the normal and shear stress components of the tidal stress tensor. For a more careful analysis of the relationship between the tidal stress tensor and the semidiurnal LFE rate modulation, we direct the interested reader to previous studies (10, 12).

The semidiurnal phase is calculated following ref. 1. We high-pass filter the calculated tidal shear stress (two-pole Butterworth, 12-h corner). This filtering damps out the fortnightly signal, and ensures that there is a well-defined minimum and maximum for each semidiurnal cycle. The distribution of the semidiurnal phase, so defined, is not entirely uniform for random times (Fig. S1). We therefore normalize the semidiurnal LFE rate histogram (Fig. 2) by the baseline distribution in Fig. S1; this is for plotting purposes only. The fluctuations in the baseline phase distribution have period equal to exactly one-half the semidiurnal period (Fig. S1), meaning there is no net contribution of this baseline nonuniformity to the cosine fit at the full semidiurnal period.

The fortnightly phase is calculated for the times of the LFEs, assuming the fortnightly amplitude is described by a cosine function with period equal to half the lunar synodic period, i.e., $2T_{fn} = 29.530589$ d. The fortnightly phase is a linear function of time $\phi_{fn} \equiv \text{mod}(\phi_0 + 360 \cdot t/T_{fn}, 360) - 180$. The amplitude $\Delta\tau = 35$ Pa/d and initial phase ϕ_0 of the fortnightly oscillation are found by stacking all of the fortnightly cycles and fitting a cosine to the 90% quantile of the shear stress. The 90% quantile is very well modeled by a cosine function, with absolute residual ≤ 2.7 Pa.

Fitting Amplitude and Phase of the Tidal Modulation. We fit the distribution of LFE phases to a cosine function by maximum likelihood. The 95% confidence range on the phase lag between tidal stress and LFE rate is defined as the range of phases for which the sample likelihood is greater than 95% of the maximum. Populations of LFEs for which 95% confidence bounds on the cosine phase do not exist are considered insignificantly different from a uniform distribution. The number of events in each LFE family is variable; this can affect the ability to resolve a significant signal, but it does not introduce systematic bias into the estimate of amplitude and phase of the modulation (Fig. S2).

We also apply Schuster's test (24) to establish significance of the tidal modulation. This test treats the occurrence of each LFE as a unit step on a

polar diagram in the direction of the instantaneous tidal phase (LFE phase). The norm of the vector sum D of these steps is a random walk in the absence of a tidal modulation. The total deviation away from the origin is a measure of the strength of the modulation, with probability $P = \exp(-D^2/N)$ of exceeding distance D by chance in N steps. Schuster's test gives no information about the phase or amplitude of the modulation but is somewhat more stringent than the 95% likelihood test. The tidal correlation for an LFE family must pass both Schuster's test ($P < 0.05$) and the 95% maximum likelihood test to be included.

LFE Catalog. We use the LFE catalog spanning the years 2008–2015, which includes ~ 4 million discrete LFEs belonging to 88 different families (19). This time period is chosen to be well outside the time affected by the 2004 Parkfield earthquake. We characterize the LFE families based on episodicity, using a metric similar to Shelly and Johnson (29), which allows us to rank LFE families according to how burst-like the activity tends to be. We define episodicity as the fraction of the total catalog duration taken up by the largest 2% of the inter-LFE times.

Statistical tests for tidal correlations assume that the LFEs are independent and identically distributed in the absence of any modulation (i.e., would be uniformly distributed). In actuality, LFEs are clustered, especially for the more episodic families. We therefore apply a simple declustering algorithm in which we count only the first LFE per family per 1-h period. The declustering limits the degree to which a single large burst can dominate the tests for significance, and allows for more precise measurements of the amplitude and phase of the tidal modulation. The declustering leaves 81,000 of the LFEs (21% of the original catalog). The major conclusions of this study do not depend on the declustering (Figs. S3 and S4).

ACKNOWLEDGMENTS. This paper benefitted from discussions with Robert Guyer, Tom Heaton, Victor Tsai, Nicholas Beeler, and Elizabeth Cochran; the latter two also provided early reviews of the manuscript. We also thank Heidi Houston, an anonymous reviewer, and editor Thorne Lay for helpful reviews and comments. This work was supported by a grant from Los Alamos National Laboratory and the US Geological Survey Mendenhall program. Any use of trade, firm, or product names is for descriptive purposes only and does not imply endorsement by the US Government.

- Tanaka S, Ohtake M, Sato H (2002) Evidence for tidal triggering of earthquakes as revealed from statistical analysis of global data. *J Geophys Res Solid Earth* 107 (B10):2211.
- Cochran ES, Vidale JE, Tanaka S (2004) Earth tides can trigger shallow thrust fault earthquakes. *Science* 306(5699):1164–1166.
- Wilcock WS (2001) Tidal triggering of microearthquakes on the Juan de Fuca Ridge. *Geophys Res Lett* 28(20):3999–4002.
- Stroup D, Bohnenstiehl D, Tolstoy M, Waldhauser F, Weekly R (2007) Pulse of the seafloor: Tidal triggering of microearthquakes at 9° 50'N East Pacific Rise. *Geophys Res Lett* 34(15):L15301.
- Métivier L, et al. (2009) Evidence of earthquake triggering by the solid Earth tides. *Earth Planet Sci Lett* 278(3):370–375.
- Gomberg J, et al. (2008) Widespread triggering of nonvolcanic tremor in California. *Science* 319(5860):173.
- Lambert A, Kao H, Rogers G, Courtier N (2009) Correlation of tremor activity with tidal stress in the northern Cascadia subduction zone. *J Geophys Res Solid Earth* 114(B8):B00A08.
- Nakata R, Suda N, Tsuruoka H (2008) Non-volcanic tremor resulting from the combined effect of Earth tides and slow slip events. *Nat Geosci* 1(10):676–678.
- Rubinstein JL, La Rocca M, Vidale JE, Creager KC, Wech AG (2008) Tidal modulation of nonvolcanic tremor. *Science* 319(5860):186–189.
- Thomas AM, Nadeau RM, Bürgmann R (2009) Tremor-tide correlations and near-lithostatic pore pressure on the deep San Andreas fault. *Nature* 462(7276):1048–1051.
- Rubinstein JL, Shelly DR, Ellsworth WL (2010) Non-volcanic tremor: A window into the roots of fault zones. *New Frontiers in Integrated Solid Earth Sciences*, eds Cloetingh SAPL, Nengendank J (Springer, New York), pp 287–314.
- Thomas AM, Bürgmann R, Shelly DR, Beeler NM, Rudolph ML (2012) Tidal triggering of low frequency earthquakes near Parkfield, California: Implications for fault mechanics within the brittle–ductile transition. *J Geophys Res Solid Earth* 117(B5): B05301.
- Beeler NM, Thomas AM, Bürgmann R, Shelly DR (2013) Inferring fault rheology from low-frequency earthquakes on the San Andreas. *J Geophys Res Solid Earth* 118(11): 5976–5990.
- Ide S (2010) Striations, duration, migration and tidal response in deep tremor. *Nature* 466(7304):356–359.
- Ide S (2012) Variety and spatial heterogeneity of tectonic tremor worldwide. *J Geophys Res Solid Earth* 117(B3):B03302.
- Houston H (2015) Low friction and fault weakening revealed by rising sensitivity of tremor to tidal stress. *Nat Geosci* 8(5):409–415.
- Obara K (2002) Nonvolcanic deep tremor associated with subduction in southwest Japan. *Science* 296(5573):1679–1681.
- Shelly DR, Beroza GC, Ide S, Nakamura S (2006) Low-frequency earthquakes in Shikoku, Japan, and their relationship to episodic tremor and slip. *Nature* 442(7099): 188–191.
- Shelly DR, Hardebeck JL (2010) Precise tremor source locations and amplitude variations along the lower-crustal central San Andreas Fault. *Geophys Res Lett* 37(L14): L14301.
- Beeler NM, Lockner DA (2003) Why earthquakes correlate weakly with the solid Earth tides: Effects of periodic stress on the rate and probability of earthquake occurrence. *J Geophys Res Solid Earth* 108(B8):2391.
- Savage HM, Marone C (2007) Effects of shear velocity oscillations on stick-slip behavior in laboratory experiments. *J Geophys Res* 112(B2):B02301.
- Hartzell S, Heaton T (1989) The fortnightly tide and the tidal triggering of earthquakes. *Bull Seismol Soc Am* 79(4):1282–1286.
- Bhatnagar T, Tolstoy M, Waldhauser F (2016) Influence of fortnightly tides on earthquake triggering at the East Pacific Rise at 9°50'N. *J Geophys Res Solid Earth* 121(3):1262–1279.
- Schuster A (1897) On lunar and solar periodicities of earthquakes. *Proc R Soc London* 61(369-377):455–465.
- Murray J, Langbein J (2006) Slip on the San Andreas Fault at Parkfield, California, over two earthquake cycles, and the implications for seismic hazard. *Bull Seismol Soc Am* 96(4B):5283–5303.
- Johnson LR, Nadeau RM (2002) Asperity model of an earthquake: Static problem. *Bull Seismol Soc Am* 92(2):672–686.
- Schmidt DA, Gao H (2010) Source parameters and time-dependent slip distributions of slow slip events on the Cascadia subduction zone from 1998 to 2008. *J Geophys Res Solid Earth* 115(B4):B00A18.
- Agnew DC (2012) *SPOTL: Some Programs for Ocean-Tide Loading* (Scripps Inst Oceanogr, San Diego).
- Shelly DR, Johnson KM (2011) Tremor reveals stress shadowing, deep postseismic creep, and depth-dependent slip recurrence on the lower-crustal San Andreas fault near Parkfield. *Geophys Res Lett* 38(13):L13312.